http://dx.doi.org/10.5012/bkcs.2014.35.10.2895

Improved Performance of CdS/CdTe Quantum Dot-Sensitized Solar Cells Incorporating Single-Walled Carbon Nanotubes

Hokyeong Shin, Taehee Park, Jongtaek Lee, Junyoung Lee, Jonghee Yang, Jin Wook Han,* and Whikun Yi*

Department of Chemistry, College of Natural Science, Hanyang University, Seoul 133-791, Korea
**E-mail: jwhan@hanyang.ac.kr (J. W. Han); wkyi@hanyang.ac.kr (W. Yi)*
Received March 25, 2014, Accepted June 3, 2014

We fabricated quantum dot-sensitized solar cells (QDSSCs) using cadmium sulfide (CdS) and cadmium telluride (CdTe) quantum dots (QDs) as sensitizers. A spin coated TiO_2 nanoparticle (NP) film on tin-doped indium oxide glass and sputtered Au on fluorine-doped tin oxide glass were used as photo-anode and counter electrode, respectively. CdS QDs were deposited onto the mesoporous TiO_2 layer by a successive ionic layer adsorption and reaction method. Pre-synthesized CdTe QDs were deposited onto a layer of CdS QDs using a direct adsorption technique. CdS/CdTe QDSSCs had high light harvesting ability compared with CdS or CdTe QDSSCs. QDSSCs incorporating single-walled carbon nanotubes (SWNTs), sprayed onto the substrate before deposition of the next layer or mixed with TiO_2 NPs, mostly exhibited enhanced photo cell efficiency compared with the pristine cell. In particular, a maximum rate increase of 24% was obtained with the solar cell containing a TiO_2 layer mixed with SWNTs.

Key Words : Quantum dot-sensitized solar cell, CdTe, CdS, Single-walled carbon nanotube

Introduction

As a third-generation photovoltaic cell, quantum dot-sensitized solar cells (QDSSCs) have been studied by many research groups due to their low production cost and high energy conversion efficiency.[1] Typical QDSSCs consist of a QD-modified photo-anode (working electrode) and a counter electrode (CE) separated by a salt electrolyte. QDs, which are nanoparticles made of semiconductor materials whose physical and chemical characteristics are size dependent, have been introduced as sensitizing materials because of their excellent opto-electronic properties. Notable properties of QDs include tunability of band gap energy, narrow emission spectrum, broad excitation spectrum, good photostability, high extinction coefficient, and multiple exciton generation (MEG).[1,2] Over the past few years, cadmium chalcogenide (CdX, X=S, Se or Te) QDs have attracted attention due to their distinguished properties such as easy fabrication, tunability by size control,[3,4] and efficient MEG. Specifically, CdSe and CdS are mainly used in CdX QD research.[1] CdTe with a bulk energy band gap of 1.54 eV is well matched with the solar light spectrum,[5] which indicates that the light-absorption of CdTe would extend to the near infrared region and that the electron injection rate from CdTe QDs to TiO_2 would be faster than CdSe QDs of the same size.[6] CdTe has the second highest extinction coefficient among CdX QDs,[7] with CdS having the highest extinction coefficient. Bulk CdS has a band gap of 2.34 eV and a relatively conductive band edge of –4.14 eV.[8] Therefore, CdS energy bands form a cascade structure with TiO_2 and CdTe energy bands. An appropriate cascade structure helps enhance the separation of electron-hole pairs.[9,10] Additionally, a CdS/CdTe co-sensitizer would have an advantage of enhancing light harvesting capability.[11]

For CdX QDSSCs, sulfide/polysulfide (S^{2-}/S_n^{2-}) is commonly used as the electrolyte. Sulfide ions are capable of scavenging photo-generated holes, and the presence of polysulfide electrolyte is necessary for the stability of metal chalcogenide-based QDSSCs.[12,13] Typically, the photo-anode consists of a mesoporous TiO_2 layer attached to the transparent conducting oxide glass.[13] In general, a Pt CE has been used in CdX QDSSCs; however, it was recently demonstrated that Au is a better CE material for QDSSCs due to its inertness. QDSSCs using Au as the CE have shown better performance compared to cells using Pt.[5,14]

Single-walled carbon nanotubes (SWNTs) have the potential to improve the performance of solar cells. In air, O_2 molecules adsorbed on the surface of SWNTs withdraw electrons, which enrich holes in SWNTs.[15] Zhong Z. and coworkers[16] reported that SWNTs act as efficient hole-transfer agents when used as a p-type semiconducting material. The use of SWNTs in solar cells could promote separation of photo-generated electron-hole pairs.

In this work, tin-doped indium oxide (ITO)/TiO_2 and fluorine-doped tin oxide (FTO)/Au film were used as the photo-anode and CE, respectively, and CdS and CdTe QDs were adopted as sensitizers of QDSSCs. The appropriate alignment of each material was designed based on consideration of the energy band edge (Fig. 1).[5,8,17] SWNTs were mixed with TiO_2 paste or were sprayed between the QD layers. The effect of SWNTs introduced into CdTe/CdS QDSSCs was studied by the photocell efficiency (PCE) and

impedance parameters.

Experimental

Preparation of CdTe QDs. CdTe QDs were synthesized following a previously reported aqueous synthesis method.[18,19] The process was comprised of three steps: preparation of NaHTe and cadmium ion solutions and growth of CdTe QDs. Te and $NaBH_4$ (molar ratio 1:4) powder were dissolved in deionized water. The mixture was placed in a refrigerator for about 2 hrs. As the chemical reaction took place, as shown below, a NaHTe solution was obtained.

$$NaBH_4 + Te + H_2O \rightarrow NaHTe + H_2 + \text{sediment}$$

For preparation of the cadmium ion solution, $CdCl_2$ was dissolved in deionized water, and thioglycolic acid (TGA) was added to the solution as a stabilizer. Freshly prepared NaHTe solution was added to the $CdCl_2$ solution, and the pH was adjusted to 11 using 1 M NaOH solution, at 100 °C under a N_2 atmosphere. The molar ratio of Cd^{2+}:TGA:HTe^- was fixed at 2:5:1. After NaHTe had been added, growth of QDs began, and different particle sizes were obtained by controlling the reflux time.

Preparation of Cell Electrodes. The porous TiO_2 photoanode was prepared by spin coating TiO_2 paste onto a 2.5 × 2.5 cm^2 ITO glass plate, followed by sintering at 450 °C for 30 min. The TiO_2 colloidal paste was prepared by mixing TiO_2 powder (Degussa P25), acetylacetone, deionized water, Triton X-100, and polyethylene glycol (PEG).[20] A successive ionic layer adsorption and reaction (SILAR) method was used to deposit CdS QDs onto the TiO_2 film.[11] The TiO_2 film was dipped into an ethanol solution containing $Cd(NO_3)_2$ (0.5 M) for 5 min followed by washing with ethanol and was then dipped for another 5 min into a Na_2S methanol solution (0.5 M) followed by washing again with methanol. These two steps were termed one SILAR cycle, and the processes were repeated 8 times followed by annealing at 400 °C for 15 min. A direct adsorption (DA) method was used to deposit CdTe QDs onto the film.[3,19] One DA cycle consisted of dipping the TiO_2/CdS film into a colloidal solution of presynthesized CdTe QDs for 30 min at 50 °C and drying in ambient atmosphere. The amount of deposited CdTe QDs was increased by repeating the cycle. The active area of the cell was 0.16 cm^2. CEs were prepared by sputtering Au onto the FTO glass.

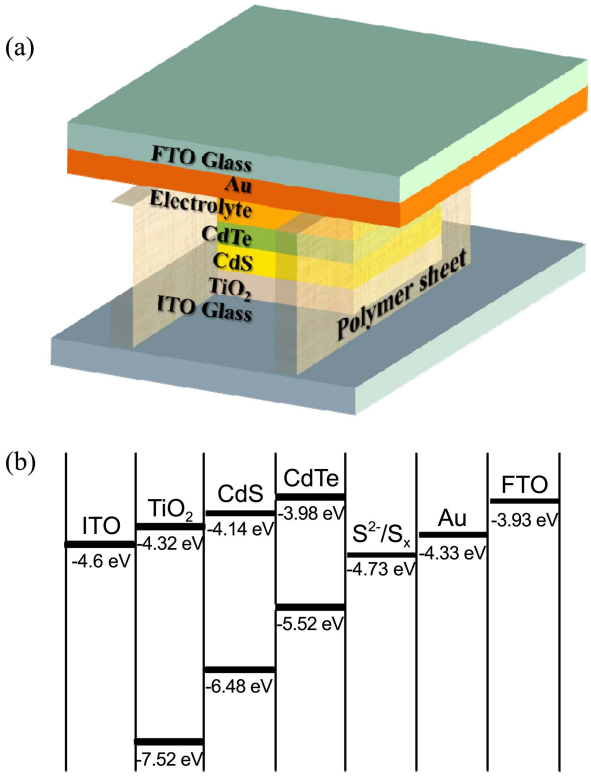

Figure 1. (a) Structure schematic and (b) energy band diagram for the CdS/CdTe quantum dot-sensitized solar cell.

Treatment of Cells Incorporating SWNTs. SWNTs were dispersed in ethanol by sonication. Two methods were used to incorporate SWNTs into cells: using a TiO_2 paste mixed with SWNTs (SWNTs/TiO_2 powder = 0.005 wt %) and spraying SWNTs (SWNTs 16 μg/cm^2) onto the surfaces of the CdS and CdTe QD layers and the Au CE.

Assembly of Cells. The photo-anode and Au CE were sandwiched between 100 μm thick polymer sheets in order to prevent evaporation of the electrolyte. Polysulfide electrolyte solution was prepared by dissolving Na_2S (0.5 M), S powder (0.125 M), and KCl (0.2 M) in water/methanol (volume ratio, 7:3) solution. A co-solvent was used to decrease the surface tension of the electrolyte solution, leading to smooth penetration of the electrolyte into the mesoporous TiO_2 matrix.[11] The electrolyte was inserted into the cell *via* a syringe, filling the space between the two electrodes.

Results and Discussion

Figure 2(a) shows the absorption spectrum of CdTe QDs in colloidal solution in the ultraviolet-visible light wavelength range. In the visible light area, the absorption maxima for samples 1-3 were observed at 484, 498, 515 nm, respectively. A red shift of the absorption spectra was observed with increasing QD growth time. The CdTe QD size could be calculated with the following equation:[7]

$$D = (9.8127 \times 10^{-7})\lambda^3 - (1.7147 \times 10^{3})\lambda^2 + (1.0064)\lambda - (194.84)$$

in which D (nm) is the size of a CdTe QD and λ (nm) is the wavelength of the first excitonic absorption peak of each sample in the visible wavelength range. Calculated QD sizes from the equation were 1.84, 2.29 and 2.71 nm for the three samples, respectively. Consequently, a red shift occurred with increasing QD size because of the quantum confinement effect. Figure 2(b) shows typical fluorescence spectra of CdTe QDs (at an excitation wavelength of 430 nm). In the spectra, the full width at half maximum (FWHM) values of the samples were 0.26, 0.31, 0.18 eV for 40, 80 and 120 min samples, respectively, which indicates a narrow size distribution and high monodispersity for the synthesized CdTe

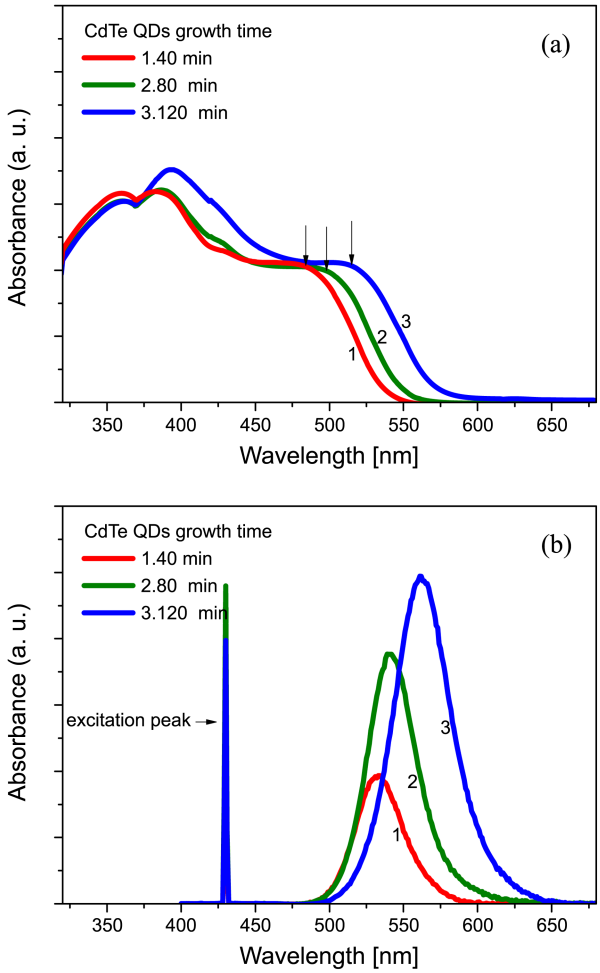

Figure 2. (a) Ultraviolet-visible light absorption and (b) photo-luminescence spectra of CdTe QDs.

QDs.[21] A 40 min QD growth time was used for our experiment samples because the driving force for faster injection of electrons into TiO_2 increased as the size of the QDs decreased.[3]

The scanning electron microscope (SEM) image in Figure 3(a) shows a compact surface layer for the TiO_2/CdS(8)/CdTe(5) film. Cd and Te characteristic peaks are clearly seen in the energy dispersive spectrum in Figure 3(b), which confirms that CdTe QDs successfully assembled on the surface of the TiO_2/CdS(8) film *via* the DA process.

The photo-current density-voltage (*J-V*) curves of different cell types are shown in Figure 4. The shapes of the *J-V* curves for CdS/CdTe QDSSCs were concave upwards, which indicates that the contact resistance between the CdS and CdTe layers was quite large. In fact, the CdS/CdTe structure has significant structural defects at the interface.[22] The combination of CdS/CdTe is structurally imperfect, but CdS/CdTe QDSSCs displayed high cell performance compared to the cell containing only CdTe as a sensitizer. Although the cell without CdS had a relatively low efficiency, the concave downwards curve suggests that the cell has a low contact resistance.

Performance parameters (open circuit voltage (V_{oc}), short

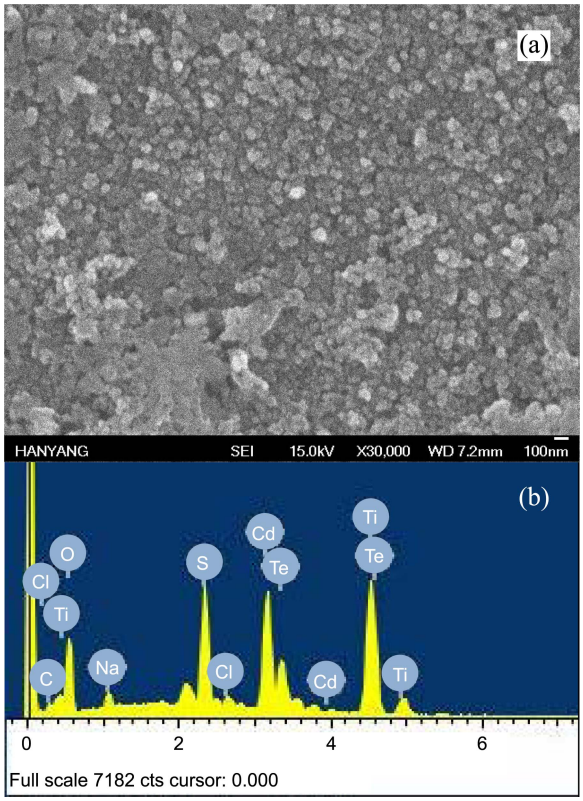

Figure 3. (a) SEM image and (b) Energy-dispersive X-ray spectroscopy spectrum of TiO_2/CdS(8)/CdTe(5) film.

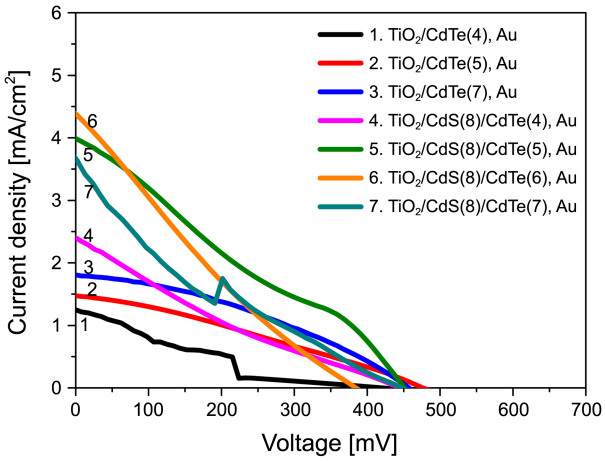

Figure 4. *J-V* curves of different cell types. The cells have co-sensitive or different deposition cycles.

circuit current density (J_{sc}), fill factor (*FF*), and PCE (η)) of the cells are listed in Table 1. As mentioned above, because of structural mismatch between CdS and CdTe, FF values of the cell with only CdTe was mostly higher than that of the CdS/CdTe cell. The PCE of CdS/CdTe QDSSCs was higher than for CdTe QDSSCs, which was evident by comparing the incident photon to current efficiency (IPCE) spectra (Figure 5) for the cells. The cell with only CdS had a broad, low intensity, and the cell with only CdTe had a high, narrow intensity. Thus, light harvesting ability was best accomplished with a combination of CdS and CdTe, as manifest by

Table 1. *J-V* curve parameters of cells with CdTe QD sensitizer or CdS/CdTe co-sensitizer with different deposition cycles

Composition	J_{sc} (mA/cm^2)	V_{oc} (mV)	*FF* (%)	η (%)
1. TiO_2/CdTe(4), Au	1.25	422	19.33	0.1016
2. TiO_2/CdTe(5), Au	1.47	467	28.97	0.2032
3. TiO_2/CdTe(7), Au	3.31	457	36.49	0.3009
4. TiO_2/CdS(8)/CdTe(4), Au	2.40	445	20.22	0.2158
5. TiO_2/CdS(8)/CdTe(5), Au	3.99	436	24.42	0.4394
6. TiO_2/CdS(8)/CdTe(6), Au	4.38	384	21.14	0.3561
7. TiO_2/CdS(8)/CdTe(7), Au	3.67	447	21.42	0.3513

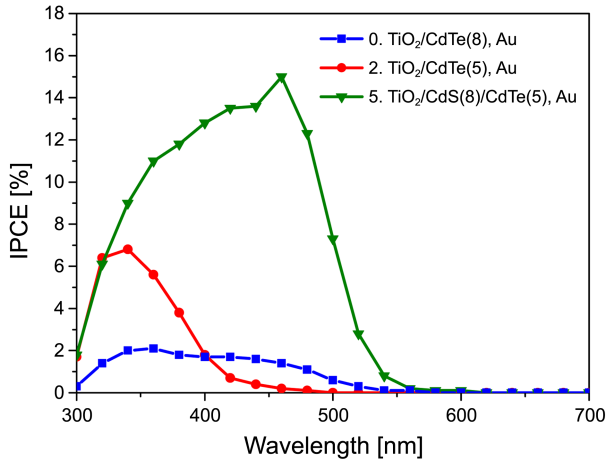

Figure 5. IPCE spectra of cells with CdS or CdTe or both as sensitizer.

the enhanced spectrum profile for TiO_2/CdS(8)/CdTe(5). Because of this harvesting ability, J_{sc} values of CdS/CdTe cell was higher than that of cell with only CdTe.

The performance of QDSSCs depended on the deposition cycles for preparing the photo-anode. An effect of the DA cycle on device performance was studied, and an optimum number of cycles was found for CdTe QDs. As the deposition cycles were increased, the PCE of the cell also generally increased. However, the PCE with CdTe QDs decreased with greater than 5 DA cycles. An increase in deposition cycles corresponded to a greater thickness of CdTe QDs. As the thickness of the CdTe layer became too thick, diffusion of charge carriers became difficult and recombination more readily occurred. A photo-anode prepared using 5 DA cycles of CdTe exhibited the best performance in our experiments.

Figure 6 shows *J-V* curves of CdS/CdTe QDSSCs containing SWNTs, and their parameters are listed in Table 2.

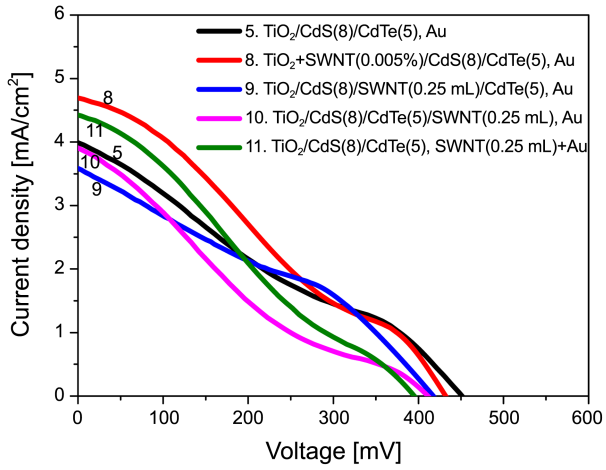

Figure 6. *J-V* curves of cells with SWNTs.

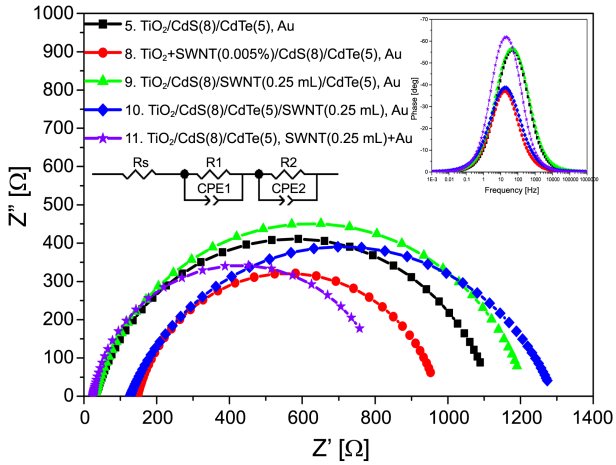

Figure 7. Nyquist plots of cells with SWNTs. Insets represent the circuit model of our cell and Bode plots, respectively.

Samples containing SWNTs had higher PCE values compared with the pristine cell (TiO_2/CdS(8)/CdTe(5)), except for the cell with SWNTs sprayed on the CdTe layer.

The increase in PCE was clearly caused by the increase in FF or J_{sc} values or both, which means that SWNTs act as excellent carrier transfer agents. The PCE of the cell with SWNTs sprayed on the CdS layer increased with increased FF despite a decreased J_{sc}. The SWNT film has a band gap of 0.6 eV with conduction and valence band energies at −4.8 and −5.4 eV *vs.* vacuum, respectively.[17] Thus, the presence of SWNTs between the CdS and CdTe layers was not appropriate from an energetic point of view, and it was possible to predict that SWNTs would act as barriers, as

Table 2. *J-V* curve parameters for the cell with SWNTs and the pristine cell

Composition	J_{sc} (mA/cm^2)	V_{oc} (mV)	*FF* (%)	η (%)
5. TiO_2/CdS(8)/CdTe(5), Au	3.99	436	24.42	0.4394
8. TiO_2+SWNT(0.005%)/CdS(8)/CdTe(5), Au	4.69	432	26.97	0.5469
9. TiO_2/CdS(8)/SWNT(0.25mL)/CdTe(5), Au	3.59	417	33.24	0.4973
10. TiO_2/CdS(8)/CdTe(5)/SWNT(0.25mL), Au	3.91	411	20.33	0.3269
11. TiO_2/CdS(8)/CdTe(5), SWNT(0.25mL)+Au	4.42	395	25.11	0.4521

Table 3. EIS spectral parameters

Composition	R_s (Ω)	R_2 (Ω)	CPE2 (F)	f_{max} (Hz)	τ_e (s)
5. TiO_2/CdS(8)/CdTe(5), Au	38.54	1069	3.11×10^{-6}	47.9	3.32×10^{-3}
8. TiO_2+SWNT(0.005%)/CdS(8)/CdTe(5), Au	136.3	856.5	1.09×10^{-5}	17	9.36×10^{-3}
9. TiO_2/CdS(8)/SWNT(0.25mL)/CdTe(5), Au	33.89	1192	2.79×10^{-6}	47.9	3.32×10^{-3}
10. TiO_2/CdS(8)/CdTe(5)/SWNT(0.25mL), Au	126.5	1166	6.53×10^{-6}	20.9	7.62×10^{-3}
11. TiO_2/CdS(8)/CdTe(5), SWNT(0.25mL)+Au	24.5	808.9	9.41×10^{-6}	20.9	7.62×10^{-3}

demonstrated by the reduction of J_{sc} for such cells compared with the pristine cell. However, as mentioned above, contact resistance between the CdS and CdTe layers was poor, and the presence of SWNTs could partially make up for the contact resistance, leading to an increase in FF, a reason for the increase in PCE. Only the cell with SWNTs sprayed on the CdTe layer exhibited a decrease in PCE compared with the pristine cell. In this case, all of the factors decreased, which suggests that SWNTs largely act as barriers in the cell. In cells with SWNTs sprayed on the Au CE or cells containing TiO_2 mixed with SWNTs, significant increases in J_{sc} and *FF* values were observed, a reflection of SWNTs acting as good carrier transfer agents at each electrode.

In addition, characterization of QDSSCs could be more rigorously analyzed using impedance data. Figure 7 and Table 3 show electrochemical impedance spectroscopy (EIS) spectra and the details for each solar cell, respectively. All of the plots exhibited Gerischer impedance, indicating low charge recombination resistance.[23] In fact, resistance between the CE and electrolyte (R_1) was not calculated from the EIS analysis program because the resistance of the active layers (R_2) was relatively large. The plots ranging from 100 KHz to 1 Hz provided information about charge transfer between layers. In the Gerischer model, the smaller semicircle represents lower resistance of active layers. Both the cell containing TiO_2 mixed with SWNTs and the cell with SWNTs sprayed on the Au CE clearly show smaller semicircles compared with the pristine cell. And both the cell with SWNTs sprayed on the CdS layer and the cell with SWNTs sprayed on the CdTe layer show slightly larger semicircles compared with the pristine cell due to resistance by SWNTs to acting as barriers.

The f_{max} values were obtained from Bode plots, and capacitance values (constant-phase elements (CPE2)) were calculated from the formula, $CPE2=1/2\pi f_{max}R_2$. The cell containing TiO_2 mixed with SWNTs had the largest capacitance and the cell with SWNTs sprayed on the CdTe layer, which had worst performance, had the smallest capacitance.

As noted above, spraying SWNTs on the CdS layer was energetically unfavorable. This finding was confirmed by the increase in the R_2 value. On the other hand, both the cell containing TiO_2 mixed with SWNTs and the cell with SWNTs sprayed on the Au CE show the decrease in the R_2 values, which indicate that SWNTs acting as good carrier transfer lowered the resistance of the active layers.

In the cell containing TiO_2 mixed with SWNTs, SWNTs could act as barriers due to the increased resistance of TiO_2 itself (R_s). However, the PCE increased with the increase in J_{sc}, indicating that SWNTs could also act as good carrier transfer agents.

Consequently, SWNTs can act as either barriers or excellent carrier transferers. In the cell containing TiO_2 mixed with SWNTs, the ability of SWNTs to act as carrier transfer agents surpassed their barrier effect. The cell also had a long electron lifetime (τ_e), which indicates a low recombination rate of carriers between electrodes. The cell with SWNTs sprayed on the Au CE also had a long electron lifetime compared with pristine cell. The cell with SWNTs sprayed on the CdTe layer had an increased R_2 value and the PCE decreased from reduction of the FF value; however, the electron lifetime of the cell increased. In this cell, electron-hole pairs were relatively well separated, but resistance in the cell could be high. Although cells with SWNTs sprayed on the CdTe layer or the Au CE had the same electron lifetimes and SWNTs present in the electrolyte, the presence of SWNTs between CdTe and the electrolyte made SWNTs act as barriers. In other words, though electron-hole pairs were well separated by presence of SWNTs, cell performance could depend on where SWNTs were in the cell.

Conclusion

CdS/CdTe QDSSCs were fabricated by SILAR and DA methods. In addition, application of SWNTs in cells was assessed for performance improvement. SWNTs could act as either a barrier or excellent carrier transfer agents and when the ability of SWNTs to act as carrier transfers surpassed their barrier effect, cell performance could be improved. With the exception of the cell with SWNTs sprayed on the CdTe layer, the performances of the other cell fabrications improved. In particular, the cell containing TiO_2 mixed with SWNTs exhibited a 24% increase in PCE compared with the pristine cell, which suggests that SWNTs acted as good carrier transfer agents that enhanced the performance of the solar cell. We expect that various applications of SWNTs to cell fabrication could be a significant factor in improving performance parameters such as energy level and resistance.

Acknowledgments. This study was supported by the National Research Foundation of Korea funded by the Ministry of Education, Science, and Technology (2011-0028850).

References

1. Jun, H. K.; Careem, M. A.; Arof, A. K. *Renewable and Sustainable Energy Reviews* **2013**, *22*, 148-167.
2. Nozik, A. J. *Chemical Physics Letters* **2008**, *457*, 3-11.
3. Badawi, A.; Al-Hosiny, N.; Abdallah, S.; Negm, S.; Talaat, H. *Solar Energy* **2013**, *88*, 137-143.
4. Lekha, P.; Balakrishnan, A.; Subramanian, K. R. V.; Nair, S. V. *Materials Chemistry and Physics* **2013**, *141*, 216-222.
5. Bang, J. H.; Kamat, P. V. *ACS Nano* **2009**, *3*(6), 1467-1476.
6. Yu, X. Y.; Lei, B. X.; Kuang, D. B.; Su, C. Y. *Chem. Sci.* **2011**, *2*, 1396.
7. Yu, W. W.; Qu, L.; Guo, W.; Peng, X. *Chem. Mater.* **2003**, *15*, 2854-2860.
8. Oladeji, I. O.; Chow, L.; Ferekides, C. S.; Viswanathan, V.; Zhao, Z. *Solar Energy Materials & Solar Cells* **2000**, *61*, 203-211.
9. Chen, M. C.; Liaw, D. J.; Huang, Y. C.; Wu, H. Y.; Tai, Y. *Solar Energy Materials & Solar Cells* **2011**, *95*, 2621-2627.
10. Wang, C.; Jiang, Z.; Wei, L.; Chen, Y.; Jiao, J.; Eastman, M.; Liu, H. *Nano Energy* **2012**, *1*, 440-447.
11. Lee, Y. L.; Lo, Y. S. *Adv. Funct. Mater.* **2009**, *19*, 604-609.
12. Lee, Y. L.; Chang, C. H. *Journal of Power Sources* **2008**, *185*, 584-588.
13. Vogel, R.; Weller, H. *J. Phys. Chem.* **1994**, *98*, 3183-3188.
14. Yeh, M. H.; Lin, L. Y.; Lee, C. P.; Chou, C. Y.; Tsai, K. W.; Lin, J. T.; Ho, K. C. *Journal of Power Sources* **2013**, *237*, 141-148.
15. Bockrath, M.; Hone, J.; Zettl, A.; McEuen, P. L.; Rinzler, A. G.; Smalley, R. E. *Physical Review B* **2000**, *61*(16), R10606.
16. Dissanayake; Nanditha, M.; Zhong, Z. *Nano Lett.* **2011**, *11*, 286-290.
17. Unalan, H. E.; Hiralal, P.; Kuo, D.; Parekh, B.; Amaratunga, G.; Chhowalla, M. *J. Mater. Chem.* **2008**, *18*, 5909-5912.
18. McSwalec, L. *Synthesis of CdTe Quantum Dots*; Diss. Worcester Polytechnic Institute, 2011.
19. Yue, G.; Wu, J.; Xiao, Y.; Lin, J.; Huang, M.; Lan, Z.; Fan, L. *Electrochimica Acta* **2012**, *85*, 182-186.
20. Arabatzis, I. M.; Antonaraki, S.; Stergiopoulos, T.; Hiskia, A.; Papaconstantinou, E.; Bernard, M. C.; Falaras, P. *Journal of Photochemistry and Photobiology A: Chemistry* **2002**, *149*, 237-245.
21. Xing, B.; Li, W. W.; Sun, K. *Materials Letters* **2008**, *62*, 3178-3180.
22. Dhere, R. G. *Study of the CdS/CdTe Interface and its Relevance to Solar Cell Properties*; Diss: 1997.
23. Fabregat-Santiago, F.; Garcia-Belmonte, G.; Mora-Seró, I.; Bisquert, J. *Phys. Chem. Chem. Phys.* **2011**, *13*, 9083-9118.